

Dissipative Distillation of Supercritical Quantum Gases

Jorge Mellado Muñoz¹, Xi Wang, Thomas Hewitt, Anna U. Kowalczyk, Rahul Sawant¹, and Giovanni Barontini^{1*}
Midlands Ultracold Atom Research Centre, School Of Physics and Astronomy, University of Birmingham, Edgbaston, Birmingham B15 2TT, United Kingdom

 (Received 5 January 2020; accepted 22 June 2020; published 8 July 2020)

We experimentally realize a method to produce nonequilibrium Bose-Einstein condensates with condensed fraction exceeding those of equilibrium samples with the same parameters. To do this, we immerse an ultracold Bose gas of ^{87}Rb in a cloud of ^{39}K with substantially higher temperatures, providing a controlled source of dissipation. By combining the action of the dissipative environment with evaporative cooling, we are able to progressively distil the nonequilibrium Bose-Einstein condensate from the thermal cloud. We show that by increasing the strength of the dissipation it is even possible to produce condensates above the critical temperature. We finally demonstrate that our out-of-equilibrium samples are long lived and do not reach equilibrium in a time that is accessible for our experiment. Due to its high degree of control, our distillation process is a promising tool for the engineering of open quantum systems.

DOI: 10.1103/PhysRevLett.125.020403

Although ubiquitous in physics, dissipation is usually considered a detrimental mechanism, as it can hinder or interfere with the behavior of the system under investigation. Notable examples are the friction that limits the performance of classical engines or the decoherence that destroys purely quantum effects. Recently it has been however realized that, if properly tamed, dissipation can be used to generate new states of matter [1–4], manipulate qubits [5], engineer decoherence-free subspaces [6–8], generate entangled quantum states [9], and distil quantum features [10]. In particular, when used to drive a system out of equilibrium, dissipation can help in reaching regions of the parameter space that are not accessible to systems in equilibrium [11,12]. In the last decades, a large effort has been put in understanding how nonequilibrium many-body systems are created and how they evolve [13,14]. In particular, the tools developed for ultracold atoms have made it possible to experimentally study the dynamics of a wide range of nonequilibrium systems including low dimensional Bose gases [15–17], quenched quantum gases [11,18,19] and prethermalized states [14,20].

In this Letter, we study the creation of supercritical nonequilibrium Bose-Einstein condensates (BECs) by combining the action of a dissipative environment with evaporative cooling, a process that we refer to as “distillation.” To this end, we immerse an ultracold cloud of ^{87}Rb at temperatures below 500 nK, within a magneto optical trap (MOT) of ^{39}K atoms at a temperature of ≈ 1 mK. This causes a loss of Rb atoms with a rate that can be controlled (Fig. 1). We find that the distillation produces long-lived out-of-equilibrium states where the condensed fraction is significantly above the equilibrium value, and even allows us to realize BECs at temperatures higher than the critical temperature. In addition, we show

that the distillation prepares the system into quasistationary nonequilibrium states that do not reach equilibrium in a time that is accessible for our experiment, therefore exhibiting the features of prethermalized states.

For an interacting Bose gas in equilibrium in a three-dimensional harmonic trap, the condensed fraction as a function of temperature obeys [21,22]:

$$F = \frac{N_0}{N} = \begin{cases} 1 - \tau^3 - \eta\tau^2(1 - \tau^3)^{2/5} & \text{for } T < T_c \\ 0 & \text{for } T > T_c \end{cases} \quad (1)$$

where T is the temperature of atomic cloud, $T_c = 0.94\hbar\omega N^{1/3}/k_B$ is the critical temperature, $\tau = T/T_c$, N_0

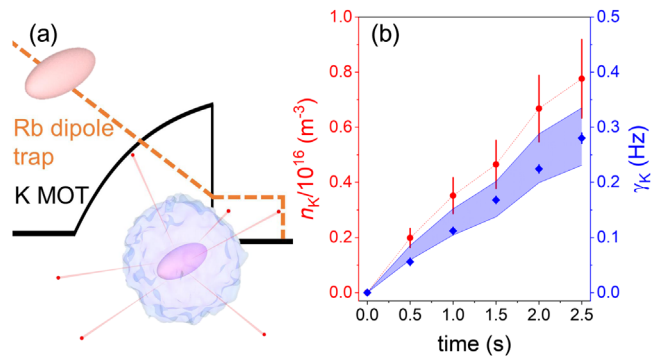


FIG. 1. (a) Schematic representation of the distillation protocol. During the last stages of the ^{87}Rb evaporative cooling, we switch on a MOT of ^{39}K . This results in the creation of a controlled dissipative environment for the Rb atoms. (b) The red dots are the measured densities of the ^{39}K atoms in the MOT as a function of time. The blue diamonds are the corresponding measured dissipation rates while the blue shaded area is the dissipation rate calculated with the model explained in the text. Error bars are the standard errors of the mean.

the number of atoms in the BEC, N the total number of atoms, ω the geometric average of the trapping frequencies, and $\eta = 2.15(aN^{1/6}/a_{\text{ho}})^{2/5}$, with a as the s -wave scattering length, $a_{\text{ho}} = (\hbar/m\omega)^{1/2}$ the harmonic trap length and m the mass of the atoms. In general, in dilute gas experiments neither ω nor N are constant as the evaporative cooling removes the more energetic atoms from the trap. In optical dipole traps, this also implies a reduction of the trapping frequencies [23]. This in turn leads to lower values of T_c as the evaporation proceeds. Both the reduction of N and ω are however very mild at the end of an optimized evaporation and Eq. (1) is usually valid with very good approximation for the vast majority of experiments [24]. In general, from Eq. (1) it follows that dissipating atoms from the system should result in a reduction of F , at least for a cloud in thermal equilibrium. However, this might not be the case if the gas is brought out of equilibrium. Under certain conditions, it might indeed happen that a quench in some of the system's parameters leads to long-lived metastable states where F exceeds the value predicted by Eq. (1), like, e.g., in [11] where a superheated BEC was realized.

In our experiment, we collect and precool the atoms in a two-species 2D MOT of Rb and K. Using a bichromatic beam of light, we then push the atoms from the 2D MOT chamber into the science chamber, where we load the overlapping 3D MOTs of Rb and K. Typically, we trap and cool $\approx 10^9$ Rb atoms at a temperature of 300 μK and $\approx 10^7$ K atoms at a temperature of 1 mK. For the experiments described in this Letter, we start by loading only the Rb 3D MOT. We subsequently load the Rb atoms directly from the MOT into an optical dipole trap formed by crossing, at an angle of ≈ 40 degrees, two beams of wavelength 1070 and 1550 nm, with waist sizes of 35 and 45 μm , respectively. Once the atoms are loaded in the dipole trap, we switch off the MOT magnetic field gradient and beams, and evaporatively cool the atoms down to the degenerate regime in 10 s. In the last 6 s of the evaporation we switch on again the MOT magnetic field gradient and obtain a BEC with 3×10^4 atoms in the $|F = 1, m_F = -1\rangle$ state. The final trapping frequencies are $\approx 2\pi \times (70, 120, 120)$ Hz. Unless otherwise stated, at the end of the sequence we hold the atoms for 20 ms in the dipole trap before releasing them and taking absorption images in time of flight.

As shown in Fig. 1, to immerse the ultracold Rb gas in a dissipative environment, we switch on the K MOT during the last stage of the evaporation, when the Rb temperature is below 1 μK , for a variable amount of time. To this end it is sufficient to switch on the K push and MOT beams, as the quadrupole magnetic field is already on. In Fig. 1(b) we report the growth of K atom density n_K as a function of the loading time (red circles). In the same figure, we report the corresponding dissipation rate γ_K as measured in our experiment (blue diamonds). As the temperature of the K atoms is ≈ 1 mK, more than three orders of magnitude

higher than the temperature of the Rb gas and the dipole trap depth, most of the collisions between K and Rb lead to the loss of Rb atoms from the dipole trap. Indeed the measured γ_K coincides with the value obtained with $\gamma_K = n_K \sigma v_K$ (shaded area), where v_K is the average speed of the K atoms and σ is calculated using the model of [32] for collisions between ultracold atoms and background classical atoms [25]. For comparison, the Rb elastic scattering rate γ_{el} , that is responsible for the thermalization of the Rb cloud, ranges between ≈ 10 –65 Hz for the experiments reported here.

In Fig. 2 we report the typical temporal evolution of the parameters of the Rb gas across the BEC transition with and without the dissipation. For the reported data, the K MOT is switched on 2 s before the end of the evaporation, where we set $t = 0$. For a direct comparison, the reported data without dissipation are chosen to approximately match the conditions with dissipation at $t = 1$ s, right before the onset of the BEC. As expected, when the dissipation is present we observe that the number of atoms is decreasing at a faster rate than the optimized evaporation [Fig. 2(a)]. Crucially, the evaporation selectively removes only the more energetic atoms from the cloud, while the dissipation coming from the K MOT is uniform and acts equally on all the velocity classes. This is reflected also in the behavior of the temperature [Fig. 2(b)], which does not change substantially when

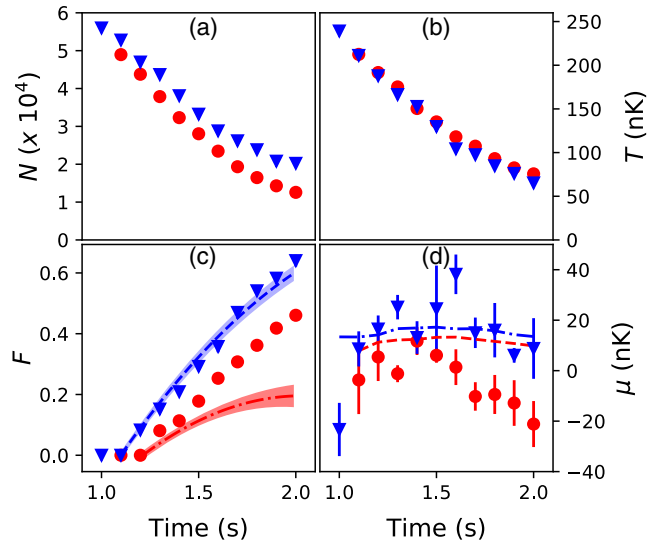


FIG. 2. Measured parameters of the ^{87}Rb sample as a function of time. Red circles are with dissipation (distillation) and blue triangles are without dissipation. (a) The total number of atoms. (b) The temperature. (c) The condensate fraction F . The red dotted dashed line and the blue dashed line show the expected fraction from Eq. (1) for with and without dissipation respectively [25]. (d) The chemical potential of the thermal part in units of temperature. The dashed and dash-dotted lines are the chemical potential of the BEC with and without dissipation, respectively. Error bars and the shaded regions are the standard errors of the mean.

the dissipation is present [33]. It also confirms that the action of the K MOT is purely dissipative (no heating) and that the dissipation does not affect the evaporative cooling and the ability of the Rb cloud to rapidly thermalize.

The corresponding measured condensed fraction F as a function of time is shown in Fig. 2(c). We observe that in the presence of the dissipation this is significantly higher than what is predicted by Eq. (1) (dashed curve). Notably, as the distillation proceeds, the discrepancy between the measured F and that predicted by Eq. (1) increases, producing a BEC substantially more pure than what can be obtained with the same atom number and temperature but without dissipation [25]. Figure 2(d) finally shows how the chemical potential of the noncondensed part of the cloud μ changes differently for with and without dissipation [25]. As expected, for both cases μ initially approaches the chemical potential of the BEC (lines). However, with distillation the behavior of μ is nonmonotonic and above $\simeq 1.5$ s reduces even when F increases, creating a system which is not in phase equilibrium [11].

In Fig. 3 we report the data as trajectories in the $F - \tau$ plane. The open symbols are the results that we obtain without dissipation, varying the initial conditions or the hold time at the end of the evaporation. The solid blue curve corresponds to Eq. (1). This demonstrate that our optimized

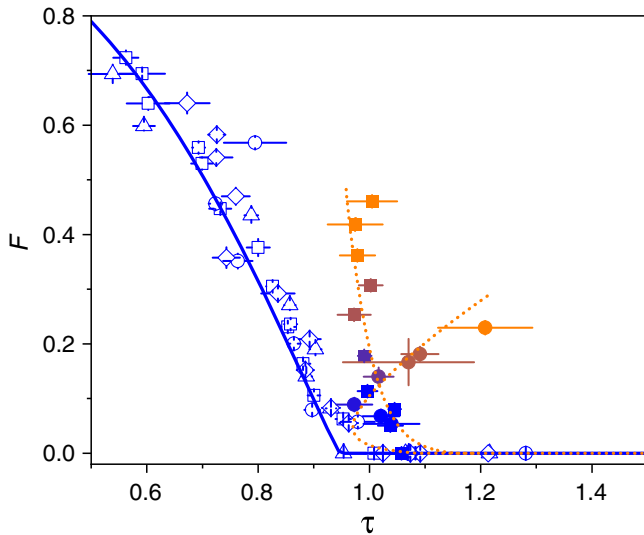


FIG. 3. Phase diagram showing the BEC fraction as a function of τ . Open symbols are for the case of no dissipation while filled symbols are the trajectories during our distillation protocol. For open diamonds and circles the wait time after the end of the evaporation ramp is 4 s, while for others it is 20 ms. For the filled circles the dissipation rate is four times the dissipation rate of the filled squares. For the data in absence of dissipation, we vary the number of atoms from 70×10^3 to 25×10^3 at $t = 1$ s in order to explore as much parameter space as possible. The solid blue line corresponds to Eq. (1). The dotted lines are the results of the rate equation model described in the text [25]. Error bars are the standard errors of the mean.

evaporation produces samples in equilibrium over a broad range of initial conditions, and that we don't need long hold times at the end of the sequence to reach equilibrium. The filled squares in Fig. 3 correspond instead to the data reported in Fig. 2. When the dissipation is switched on, the trajectory substantially differs from Eq. (1), and notably we are able to progressively distil purer samples. Our distillation allows us to explore regions of the phase diagram that are not accessible for gases in equilibrium and that feature a higher purity. We refer to those samples as “supercritical BECs.”

During the distillation, the dissipation shifts T_c to lower values, counteracting the action of the evaporation that reduces T , so that τ remains approximately constant. However, at the same time F increases, meaning that while the reduction of T pumps atoms in the BEC, the reduction of T_c is not able to depump them back into the thermal component at the same rate. As it can be observed in Fig. 3, the result is a steeper purification with distillation, and a BEC with $F \simeq 0.5$ can be produced already for $\tau \simeq 1$. This effect is even more apparent if we increase the rate of dissipation by a factor of 4 (filled circles). To do so, we increase the power of the push beam, so that the loading rate of the K MOT is quadrupled. In this case, the distillation is so effective that the trajectory *inverts* and we are able to increase F even if we increase τ .

In Fig. 4 we address the issue of the lifetime of our supercritical states. To measure the lifetime, we switch off the dissipation right after the state has been created following a trajectory similar to the one of Fig. 2. Then we keep the cloud in the dipole trap with a constant trap depth for a variable amount of time. In Fig. 4 we report the difference δF between the measured F and Eq. (1) as a function of time after the dissipation has been switched off [25]. For the first 1.5 s, the system is driven even further out of equilibrium by plain evaporation and then it slowly

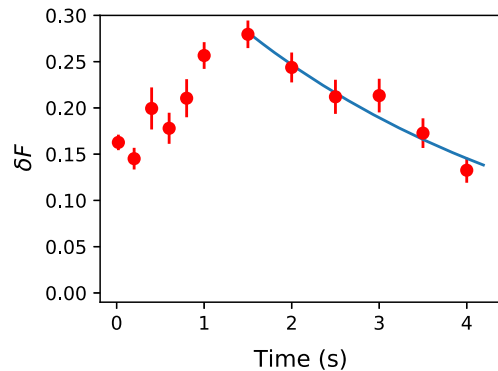


FIG. 4. Difference between the measured F and that expected using Eq. (1) after the dissipation from the K MOT is switched off and the sample is held with constant trap depth. Error bars are the standard errors of the mean. The line shows an exponential fit to the data after 1.5 seconds, when the supercritical gas relaxes towards equilibrium. The time constant is 3.9 ± 0.3 s.

relaxes toward lower values of δF . However, for as long as we can measure, δF never goes below the initial value. With respect to the typical timescales of the experiment, which range from $1/\omega \simeq 0.1$ ms to $1/\gamma_{\text{el}} \simeq 100$ ms, the relaxation dynamics can therefore be considered quasi-static, meaning that our supercritical samples possess similar properties as a prethermalized state.

The dynamics of the formation of the BEC during evaporative cooling is a complex many-body problem that can be quantitatively described with quantum kinetic theory. The solution of such a theory is however practically infeasible. A handful of works have tried to reproduce the experimental observations using some approximations, like constant temperature and infinite atom reservoir, but only with partial success [34,35]. The addition of the dissipation makes the microscopic description of our dissipative distillation an even more challenging task. A promising approach to the problem could be the stochastic phase-space method of [36], which has proven to be successful for systems of $\simeq 10^4$ atoms with vanishing interactions. Another possibility would be to extend the techniques used for the description of the nonequilibrium formation of exciton polariton condensates [37,38]. In this Letter we take instead a phenomenological approach and develop a rate equation model based on those in [11,34,35,39]. This allows us to describe our experimental data and derive important information that can be used to develop a rigorous microscopic theory. Our model describes our system as a two-mode system, with one mode being the BEC and the other the thermal component [25]:

$$\begin{aligned} \dot{N}_0 &= \bar{W} \left[\left(1 - \frac{t}{t_f}\right) N_0 + 1 \right] - \bar{K}(\tilde{N}_{\text{th}} + 1) - \gamma_K(t) N_0 \\ \dot{N}_{\text{th}} &= -\bar{W} \left[\left(1 - \frac{t}{t_f}\right) N_0 + 1 \right] + \bar{K}(\tilde{N}_{\text{th}} + 1) + \\ &\quad - [\gamma_K(t) + \gamma] N_{\text{th}}. \end{aligned} \quad (2)$$

\bar{W} and \bar{K} are respectively the growth rate of the condensate and of the thermal component and are derived from the data without dissipation. The loss rate γ accounts for the evaporative cooling while t_f for the saturation of the BEC, these parameters are also extracted from the data without dissipation. \tilde{N}_{th} is the effective number of atoms in the thermal mode and is the only free parameter of our model [25]. The results are reported as dotted lines in Fig. 3 where it can be appreciated that our model is able to reproduce fairly well the trajectories of our dissipative distillation.

The crucial element of our dissipative distillation is the fact that the rates \bar{W} , promoted by the reduction in temperature coming from the evaporative cooling, and \bar{K} , promoted by a reduction of the chemical potential coming from the dissipation, do not coincide for a Bose gas

out of equilibrium. By considering two-body collisions as the only mechanism responsible for the growth of the condensate, and using quantum kinetic theory, it is indeed possible to demonstrate that $\bar{W} \simeq \exp(\Delta/k_B T) \bar{K}$, with Δ the energy difference between the two components [25,34,35]. The energy gap can be roughly estimated from the energy spectrum obtained with a first-order treatment of a uniform Bose gas with contact interactions. For $\tau \leq 1$, this reduces to [40,41]:

$$E = \frac{p^2}{2m} + \frac{4\pi\hbar^2 a N^2}{mV} \left(1 - \frac{1}{2} F^2\right), \quad (3)$$

where p is the momentum of the atom and V the trapping volume. The last term is of quantum mechanical origin and accounts for bosonic stimulation. From Eq. (3) it follows that once an atom is in the condensed phase, it needs an amount of energy $\Delta = 2\pi\hbar^2 a N_0/mV$ to leave the BEC, yielding an unbalancing between \bar{W} and \bar{K} . More detailed calculations including higher order perturbation theory [40,41] and the effect of the mean field potential of the BEC [35,39] show that the spectrum exhibits a strong modification of the density of states right above the condensed state, therefore Eq. (3) is valid only for low values of F . Regardless, for $\tau \simeq 1$, in our experimental conditions Δ is already of the same order of magnitude as T .

In conclusion, we have implemented an open many-body quantum system by immersing an ultracold gas in a controlled dissipative environment, embodied by a cold gas of atoms of a different species. We have shown that by combining the dissipation with evaporative cooling it is possible to realize states of matter that are not accessible for equilibrium or closed systems. In particular we were able to create and grow supercritical BECs, even at temperatures higher than the critical temperature. The states created exhibit a quasistatic behavior typical of prethermalized states and can be practically used to perform experiments with high condensed fractions at high temperatures. On the one hand, our results have the potential to trigger the interest of the theory community to develop a microscopic description of out-of-equilibrium quantum gases. On the other, the ability to control the dissipation and the temperature of the sample can provide a new tool for distilling environmentally resilient states and engineering quantum phases in open quantum system.

The authors are supported by the Leverhulme Trust Research Project Grant UltraQuTe (Grant No. RGP- 2018-266). We are grateful to J. Goldwin and V. Boyer and V. Garrera for reading the manuscript and the useful comments. We acknowledge fruitful discussions with the members of the Cold Atoms Group at the University of Birmingham.

J. M. M. and R. S. contributed equally to this work.

- *g.barontini@bham.ac.uk
- [1] G. Nocolis, Dissipative systems, *Rep. Prog. Phys.* **49**, 873 (1986).
- [2] L. H. Dogra, J. A. P. Glidden, T. A. Hilker, C. Eigen, E. A. Cornell, R. P. Smith, and Z. Hadzibabic, Can Three-Body Recombination Purify a Quantum Gas?, *Phys. Rev. Lett.* **123**, 020405 (2019).
- [3] B. Buča and D. Jaksch, Dissipation Induced Nonstationarity in a Quantum Gas, *Phys. Rev. Lett.* **123**, 260401 (2019).
- [4] N. Dogra, M. Landini, K. Kroeger, L. Hruby, T. Donner, and T. Esslinger, Dissipation-induced structural instability and chiral dynamics in a quantum gas, *Science* **366**, 1496 (2019).
- [5] J. T. Barreiro, M. Müller, P. Schindler, D. Nigg, T. Monz, M. Chwalla, M. Hennrich, C. F. Roos, P. Zoller, and R. Blatt, An open-system quantum simulator with trapped ions, *Nature (London)* **470**, 486 (2011).
- [6] J. I. Cirac and P. Zoller, Quantum Computations with Cold Trapped Ions, *Phys. Rev. Lett.* **74**, 4091 (1995).
- [7] D. A. Lidar, I. L. Chuang, and K. B. Whaley, Decoherence-Free Subspaces for Quantum Computation, *Phys. Rev. Lett.* **81**, 2594 (1998).
- [8] A. Beige, D. Braun, B. Tregenna, and P. L. Knight, Quantum Computing Using Dissipation to Remain in a Decoherence-Free Subspace, *Phys. Rev. Lett.* **85**, 1762 (2000).
- [9] G. Barontini, L. Hohmann, F. Haas, J. Estève, and J. Reichel, Deterministic generation of multiparticle entanglement by quantum zeno dynamics, *Science* **349**, 1317 (2015).
- [10] K. G. H. Vollbrecht, C. A. Muschik, and J. I. Cirac, Entanglement Distillation by Dissipation and Continuous Quantum Repeaters, *Phys. Rev. Lett.* **107**, 120502 (2011).
- [11] A. L. Gaunt, R. J. Fletcher, R. P. Smith, and Z. Hadzibabic, A superheated Bose-condensed gas, *Nat. Phys.* **9**, 271 (2013).
- [12] M. H. Szymańska, J. Keeling, and P. B. Littlewood, Non-equilibrium Bose–Einstein condensation in a dissipative environment, in *Quantum Gases: Finite Temperature and Non-equilibrium Dynamics* (World Scientific, Singapore, 2013), pp. 447–459, https://doi.org/10.1142/9781848168121_0030.
- [13] A. Polkovnikov, K. Sengupta, A. Silva, and M. Vengalattore, Colloquium: Nonequilibrium dynamics of closed interacting quantum systems, *Rev. Mod. Phys.* **83**, 863 (2011).
- [14] T. Langen, R. Geiger, and J. Schmiedmayer, Ultracold atoms out of equilibrium, *Annu. Rev. Condens. Matter Phys.* **6**, 201 (2015).
- [15] T. Kinoshita, T. Wenger, and D. S. Weiss, A quantum Newton’s cradle, *Nature (London)* **440**, 900 (2006).
- [16] S. Hofferberth, I. Lesanovsky, B. Fischer, T. Schumm, and J. Schmiedmayer, Non-equilibrium coherence dynamics in one-dimensional Bose gases, *Nature (London)* **449**, 324 (2007).
- [17] S. Trotzky, Y.-A. Chen, A. Flesch, I. P. McCulloch, U. Schollwck, J. Eisert, and I. Bloch, Probing the relaxation towards equilibrium in an isolated strongly correlated one-dimensional Bose gas, *Nat. Phys.* **8**, 325 (2012).
- [18] L. E. Sadler, J. M. Higbie, S. R. Leslie, M. Vengalattore, and D. M. Stamper-Kurn, Spontaneous symmetry breaking in a quenched ferromagnetic spinor Bose-Einstein condensate, *Nature (London)* **443**, 312 (2006).
- [19] R. P. Smith, S. Beattie, S. Moulder, R. L. D. Campbell, and Z. Hadzibabic, Condensation Dynamics in a Quantum-Quenched Bose Gas, *Phys. Rev. Lett.* **109**, 105301 (2012).
- [20] M. Gring, M. Kuhnert, T. Langen, T. Kitagawa, B. Rauer, M. Schreitl, I. Mazets, D. A. Smith, E. Demler, and J. Schmiedmayer, Relaxation and prethermalization in an isolated quantum system, *Science* **337**, 1318 (2012).
- [21] F. Dalfovo, S. Giorgini, L. P. Pitaevskii, and S. Stringari, Theory of Bose-Einstein condensation in trapped gases, *Rev. Mod. Phys.* **71**, 463 (1999).
- [22] N. Tammuz, R. P. Smith, R. L. D. Campbell, S. Beattie, S. Moulder, J. Dalibard, and Z. Hadzibabic, Can a Bose Gas Be Saturated?, *Phys. Rev. Lett.* **106**, 230401 (2011).
- [23] D. Benedicto-Orenes, A. Kowalczyk, K. Bongs, and G. Barontini, Endoscopic imaging of quantum gases through a fiber bundle, *Opt. Express* **25**, 19701 (2017).
- [24] Further corrections taking into account inter-particle interactions and finite-size effects are discussed in the Supplemental Material [25].
- [25] See the Supplemental Material at <http://link.aps.org/supplemental/10.1103/PhysRevLett.125.020403> for details about the calibration of the trapping frequencies, finite size effects, the calculation of the dissipation rate, and the chemical potential and the explanation of the rate equation model, including Refs. [26–31].
- [26] V. Makhalov, K. Martiyanov, T. Barmashova, and A. Turlapov, Precision measurement of a trapping potential for an ultracold gas, *Phys. Lett. A* **379**, 327 (2015).
- [27] W. Ketterle, D. S. Durfee, and D. M. Stamper-Kurn, Making, probing and understanding Bose-Einstein condensates, [arXiv:cond-mat/9904034](https://arxiv.org/abs/cond-mat/9904034).
- [28] F. Gerbier, J. H. Thywissen, S. Richard, M. Hugbart, P. Bouyer, and A. Aspect, Critical Temperature of a Trapped, Weakly Interacting Bose Gas, *Phys. Rev. Lett.* **92**, 030405 (2004).
- [29] R. P. Smith, R. L. D. Campbell, N. Tammuz, and Z. Hadzibabic, Effects of Interactions on the Critical Temperature of a Trapped Bose Gas, *Phys. Rev. Lett.* **106**, 250403 (2011).
- [30] A. Simoni, M. Zaccanti, C. DErrico, M. Fattori, G. Roati, M. Inguscio, and G. Modugno, Near-threshold model for ultracold krb dimers from interisotope feshbach spectroscopy, *Phys. Rev. A* **77**, 052705 (2008).
- [31] H.-J. Miesner, D. M. Stamper-Kurn, M. R. Andrews, D. S. Durfee, S. Inouye, and W. Ketterle, Bosonic stimulation in the formation of a Bose-Einstein condensate, *Science* **279**, 1005 (1998).
- [32] E. A. Cornell, J. R. Ensher, and C. E. Wieman, Experiments in dilute atomic Bose-Einstein condensation, [arXiv:cond-mat/9903109](https://arxiv.org/abs/cond-mat/9903109).
- [33] The temperature of the data with dissipation is systematically higher than in absence of dissipation, this is because the evaporative cooling is less efficient as the number of atoms is reduced.
- [34] D. Jaksch, C. W. Gardiner, and P. Zoller, Quantum kinetic theory. ii. simulation of the quantum Boltzmann master equation, *Phys. Rev. A* **56**, 575 (1997).
- [35] C. W. Gardiner, M. D. Lee, R. J. Ballagh, M. J. Davis, and P. Zoller, Quantum Kinetic Theory of Condensate Growth:

- Comparison of Experiment and Theory, *Phys. Rev. Lett.* **81**, 5266 (1998).
- [36] P. D. Drummond and J. F. Corney, Quantum dynamics of evaporatively cooled Bose-Einstein condensates, *Phys. Rev. A* **60**, R2661 (1999).
- [37] I. Carusotto and C. Ciuti, Quantum fluids of light, *Rev. Mod. Phys.* **85**, 299 (2013).
- [38] H. Deng, H. Haug, and Y. Yamamoto, Exciton-polariton Bose-Einstein condensation, *Rev. Mod. Phys.* **82**, 1489 (2010).
- [39] C. W. Gardiner, P. Zoller, R. J. Ballagh, and M. J. Davis, Kinetics of Bose-Einstein Condensation in a Trap, *Phys. Rev. Lett.* **79**, 1793 (1997).
- [40] K. Huang and C. N. Yang, Quantum-mechanical many-body problem with hard-sphere interaction, *Phys. Rev.* **105**, 767 (1957).
- [41] K. Huang, C. N. Yang, and J. M. Luttinger, Imperfect Bose gas with hard-sphere interaction, *Phys. Rev.* **105**, 776 (1957).